Proc. NIPR Symp. Antarct. Geosci., 1, 129–149, 1987

BASIC AND INTERMEDIATE GNEISSES FROM THE WESTERN PART OF THE SØR RONDANE MOUNTAINS, EAST ANTARCTICA

Kazuyuki SHIRAISHI[1] and Satoru KOJIMA[2]

[1]*National Institute of Polar Research, 9–10, Kaga, 1-chome, Itabashi-ku, Tokyo 173*
[2]*Department of Earth Sciences, Nagoya University, Furo-cho, Chikusa-ku, Nagoya 464*

Abstract: This work reports the results of petrography and electron microprobe studies of minerals in basic to intermediate gneisses from the western part of the Sør Rondane Mountains. Mineral paragenesis and electron microprobe data indicate the metamorphic grade in the northern part of the study area is the granulite facies, whereas that of the southern part is the upper amphibolite facies. Estimated *P-T* conditions of peak metamorphism in the northern part of the area are around 800°C and 7–8.5 kb based on various geothermo-barometries. Widespread retrograde metamorphism caused probably by mylonitization and granite intrusion resulted in the formation of secondary minerals in both the granulite facies and the upper amphibolite facies rocks.

1. Introduction

The western part of the Sør Rondane Mountains (71.5–72.5°S, 22.5–24.5°E: Fig. 1) is underlain by metamorphic rocks probably of Late Proterozoic age, and plutonic rocks and minor dike rocks of Early Paleozoic age (VAN AUTENBOER and LOY, 1972; KOJIMA and SHIRAISHI, 1986). However, the grade of the regional metamorphism has not been clarified. VAN AUTENBOER and LOY (1972) simply stated "The metamorphism of the gneisses can be characterized as being upper catazonal and lower mesozonal with a local epizonal dynamo-retromorphism". Recently, a progressive metamorphism from the upper amphibolite to granulite facies of the medium-pressure type was established in the Prince Olav Coast and Lützow-Holm Bay region (37–45°E), eastern Queen Maud Land (*e.g.* HIROI *et al.*, 1987). Characterization of regional metamorphism in the Sør Rondane Mountains is an urgent problem to compare it with those of the other portions of East Antarctica for understanding the crustal development of the Shield.

In this study, we will examine the regional gradation of metamorphism in terms of petrographic and mineralogic characters of the basic to intermediate gneisses, and estimate the peak metamorphic conditions in the western part of the Sør Rondane Mountains, using various geothermo-barometers.

2. Geological Setting

A geologic outline and a brief description of the metamorphic and plutonic

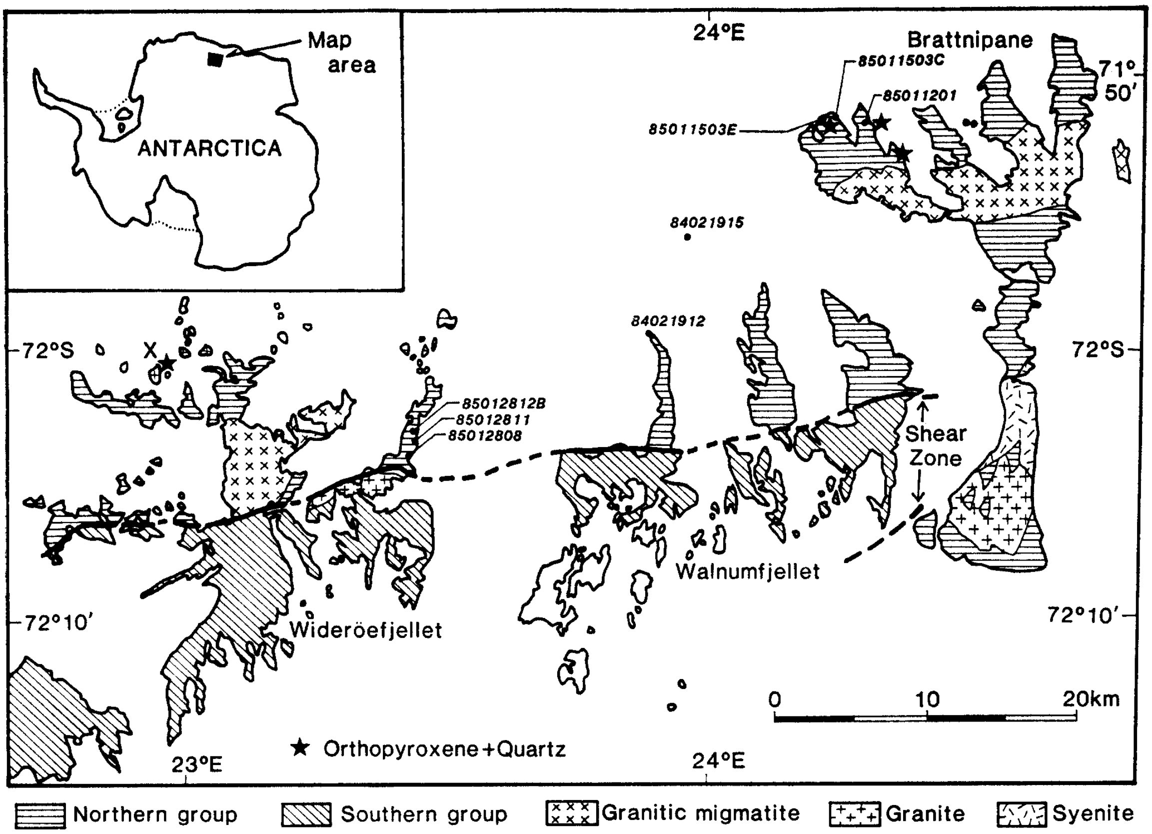

Fig. 1. Generalized geological map of the western part of the Sør Rondane Mountains. Localities of specimens described in this paper and localities of orthopyroxene+quartz assemblage are also shown. "X" denotes that the above assemblage was found from a xenolithic block in granite.

rocks in the western part of the Sør Rondane Mountains are given by KOJIMA and SHIRAISHI (1986). The area is underlain by various kinds of metamorphic and plutonic rocks (Fig. 1). Foliation of the gneisses generally trends E-W, and dips south. The metamorphic rocks are divided into two groups: the northern group consisting of pelitic, semipelitic and intermediate gneisses with subordinate amounts of basic and calcareous rocks, and the southern group composed of gneissose tonalite with fragments of basic schist and minor amounts of semipelitic schists. A pronounced shear fault (Main Shear Zone by KOJIMA and SHIRAISHI (1986)) separates the two groups. It is characteristic that intense mylonitization and cataclasis accompanied by retrograde metamorphism are widespread. Especially in the southern group, the peak metamorphic assemblages are hardly recognized. Therefore, the area where the southern group is distributed is considered to be an E-W trending tectonic belt, reaching more than 10 km wide.

Early Paleozoic plutonic rocks are granite, syenite and diorite, and form sporadic stocks and small masses throughout the region. Slightly metamorphosed andesitic* dikes whose whole-rock K-Ar age is 536±27 Ma intrude the metamorphic

* Although KOJIMA and SHIRAISHI (1986) described the rock type as dolerite, the present specimen is andesite in petrochemical sense.

rocks.

3. Mode of Field Occurrence of Specimens

Because the southern group area is considered to be a shear belt, only rocks from the northern group are examined for regional metamorphic gradation in the present study.

Mineral assemblages of the intermediate to basic rocks described in this study are shown in Table 1, and localities of the specimens are shown in Fig. 1. To examine the regional gradation of the metamorphic grade, we selected the specimens from the northern group in order of the apparent stratigraphic sequence.

Table 1. Mineral assemblages of rocks described and mineral abbreviations.

Specimen No.	Opx	Cpx	Ca-amph	Cum	Gar	Epi	Bi	Mus	Chl
85012808			+			*	+		
85012811			+			*	+	*	
85012812B			+			*	+	*	*
84021912			+		—	*	—		
84021915			+			*	+		*
85011201	+	+	+	*			—		
85011503C	+	+	+				—		
85011503E	+	+	+	*	+		—		

Specimen No.	Pl (An)	Kf	Qz	Il	Mag	Others
85012808	35–19		+		+	Sph, Apt, Sul, Hem, Zir, Cc
85012811	37–32		+		+	Cc, Apt
85012812B	27–24	+	+		—	Hem, Sph, Apt, Zir, Cc
84021912	28–23		+		—	Hem, Sph, Apt
84021915	34–29		+		—	Hem, Sph, Apt, Sul
85011201	43–30		+	+	+	Sul, Zir, Apt, Hem
85011503C	37–35		+			Hem, Sul, Apt
85011503E	38–34		+	+	+	Apt, Sul, Hem, Zir

+: present, —: rarely present, *: retrograde mineral.
Mineral abbreviations
Amph: amphibole, Apt: apatite, Bi: biotite, Cc: calcite, Chl: chlorite, Cpx: clinopyroxene, Cum: cummingtonite, Epi: epidote, Gar: garnet, Hb: hornblende, Hem: hematite, Il: ilmenite, Kf: K-feldspar, Mag: magnetite, Mus: muscovite, Opx: orthopyroxene, Pl: plagioclase, Qz: quartz, Sph: sphene, Sul: sulfide minerals, Tsch: tschermakite, Zir: zircon.

Intermediate to basic gneisses comprise hornblende gneisses and amphibolite described by KOJIMA and SHIRAISHI (1986). The hornblende gneisses of intermediate composition are the most predominant rock type in the northern group. Amphibolite occurs as a dark-band of 0.1 to a few meters wide interbedded within biotite gneisses and hornblende gneisses (Plate 1a).

Medium-grained massive sp. 85012808, 85012811 and 85012812B were collected from the Vengen ridge, the type locality of the Teltet-Vengen Group by VAN AUTENBOER and LOY (1972). In this ridge, subconcordant layers and dikes of granite and local shear zones which result in mylonitic appearance of the gneisses are abundant (Plate 1c). Sp. 85012808 occurs as an agmatized block intruded by many granite dikes. Sp. 85012812B occurs in contact with a small granite mass. It is evident that these granites caused more or less thermal effects on the country metamorphic rocks. Sps. 84021912 and 84021915 show fine banded structures of mafic and salic layers ranging from a few to several cm thick (Plate 1b).

In the northwestern part of Brattnipane, two-pyroxene-bearing hornblende gneisses are common (sps. 85011201, 85011503C and 85011503E). They are medium- to coarse-grained, dark-colored rocks, containing dark-colored feldspar and quartz which are peculiar to charnockitic rocks.

4. Mineral Textures and Chemistry

Microprobe analyses were performed using an JEOL JXA-733 analyzer at the National Institute of Polar Research, Tokyo. The analysis conditions are after the standard method at the institute, using synthesized pure oxides and natural minerals as standards with the Bence and Albee's correction method. Representative microprobe analyses are listed in Tables 2 to 7.

4.1. Pyroxenes

Orthopyroxene occurs in direct contact with clinopyroxene and calcic amphibole. Some pyroxenes are poikilitic and include quartz, magnetite and ilmenite. The Mg/(Mg+Fe) ratios of both pyroxenes are much lower in the garnet-bearing rock (85011503E) than in the garnet-free rocks, reflecting the difference in the bulk chemical composition. Orthopyroxene is ferrohypersthene and contains MnO around 1 wt%. Chemical zoning of pyroxenes is not distinct, but a slight decrease of Al_2O_3 (less than 0.6 wt%) at the rims of clinopyroxene is observed.

4.2. Amphiboles

Calcic amphibole generally shows color zoning; brownish green to dark green in the inner part and pale green to bluish green in the outer part. Core compositions are generally more titanian and alkaline than rim compositions.

Regional variation of core compositions is characteristic in the northern group area. Although the K_2O content is generally high, over 1.2 wt%, it is higher in the orthopyroxene-bearing (opx-bg.) rocks from the northern part than in the orthopyroxene-free (opxfree) rocks from the southern part. It is significant that TiO_2 contents are higher (more than 2 wt%) in the opx-bg. rocks than those in the opx-free rocks.

In the opx-bg. rocks, green calcic amphibole occurs along cracks of clinopyroxene and fringes magnetite and ilmenite (Plate 2c). Retrograde cummingtonite surrounds orthopyroxene in specimens 85011201 and 85011503E. A mantle of cummingtonite in sp. 85011201 is also surrounded by a second mantle of bluish green calcic amphibole which is highly tschermakitic in composition (Plate 2a).

Table 2. Representative microprobe analyses of pyroxenes.

Specimen No.	85011201				85011503C				85011503E			
	Cpx		Opx		Cpx		Opx		Cpx		Opx	
	core	rim	core	rim	core	rim	core	rim	core	rim	core	rim
Analysis No.	326	325	331	333	204	203	201	202	163	304	212	313
SiO_2	50.42	51.31	50.82	51.10	51.91	51.90	50.91	50.72	50.02	50.43	49.31	49.50
TiO_2	0.23	0.18	0.07	0.08	0.19	0.17	0.10	0.07	0.24	0.20	0.11	0.05
Al_2O_3	2.64	2.02	1.39	1.18	1.77	1.31	0.72	0.74	2.38	1.79	0.76	0.59
Cr_2O_3	0.04	0.00	0.04	0.04	0.00	0.04	0.06	0.00	0.00	0.01	0.00	0.01
FeO*	13.21	11.96	29.43	29.43	13.43	12.03	30.38	31.36	15.52	15.05	34.96	35.27
MnO	0.49	0.41	1.02	1.11	0.44	0.47	1.10	0.95	0.41	0.52	1.02	0.89
MgO	11.43	11.36	16.23	16.06	11.84	11.93	16.45	15.99	9.42	9.80	12.78	12.77
CaO	20.79	22.02	0.78	0.67	20.43	21.73	0.70	0.66	20.26	20.87	0.70	0.67
Na_2O	0.52	0.50	0.00	0.00	0.36	0.43	0.04	0.02	0.60	0.45	0.01	0.02
Total	99.78	99.78	99.77	99.70	100.39	100.03	100.45	100.50	98.86	99.11	99.64	99.78
On the basis of 6 oxygens												
Si	1.925	1.950	1.970	1.982	1.962	1.966	1.971	1.970	1.945	1.955	1.972	1.978
Al^{IV}	0.075	0.050	0.030	0.018	0.038	0.034	0.029	0.030	0.055	0.045	0.028	0.022
Al^{VI}	0.043	0.041	0.034	0.036	0.041	0.025	0.004	0.004	0.055	0.037	0.008	0.006
Ti	0.007	0.005	0.002	0.002	0.006	0.005	0.003	0.002	0.007	0.006	0.003	0.002
Cr	0.001	0.000	0.001	0.001	0.000	0.001	0.002	0.000	0.000	0.000	0.000	0.000
Fe	0.422	0.380	0.954	0.955	0.425	0.381	0.984	1.019	0.505	0.488	1.169	1.179
Mn	0.016	0.013	0.034	0.036	0.014	0.015	0.036	0.031	0.014	0.017	0.035	0.030
Mg	0.651	0.644	0.938	0.929	0.667	0.674	0.950	0.926	0.546	0.567	0.762	0.761
Ca	0.850	0.897	0.032	0.028	0.827	0.882	0.029	0.028	0.844	0.867	0.030	0.029
Na	0.038	0.037	0.000	0.000	0.027	0.032	0.003	0.001	0.045	0.034	0.001	0.001
Mg/(Mg+Fe)	0.607	0.629	0.496	0.493	0.611	0.639	0.491	0.476	0.520	0.537	0.395	0.392

* Total Fe as FeO.

Table 3. Representative chemical compositions of Ca-amphiboles and cummingtonites.[†]

Specimen No.	85012808		85012811		85012812B		84021912		84021915	
Analysis	core	rim	core	rim	core	rim	core	rim	core	rim
No.	302	214	210	213	110	107	201	214	310	311
SiO_2	40.43	40.55	40.95	42.79	41.50	41.99	40.48	39.30	41.30	43.11
TiO_2	1.30	0.84	1.33	1.17	1.85	1.68	1.48	0.60	1.36	0.56
Al_2O_3	11.07	11.38	11.15	11.00	10.57	10.85	10.93	12.49	11.67	10.56
Cr_2O_3	0.00	0.03	0.00	0.00	0.07	0.00	0.02	0.01	0.08	0.02
FeO*	19.65	20.37	18.44	18.66	19.59	20.02	22.74	23.04	18.93	18.05
MnO	0.77	0.83	0.48	0.34	0.34	0.32	0.66	0.46	0.54	0.50
MgO	8.60	7.85	9.24	9.15	8.36	7.98	6.49	6.35	8.75	9.48
CaO	11.44	11.39	11.20	11.22	11.67	11.52	10.89	11.41	11.48	12.05
Na_2O	1.42	1.47	1.39	1.26	1.00	0.94	1.50	1.46	1.37	1.19
K_2O	1.64	1.50	1.31	1.20	1.41	1.40	1.54	1.43	1.23	0.74
Total	96.32	96.21	95.49	96.78	96.37	96.69	96.73	96.55	96.70	96.25
On the basis of 23 oxygens										
Si	6.254	6.295	6.319	6.496	6.398	6.450	6.324	6.131	6.309	6.553
Ti	0.151	0.098	0.154	0.134	0.214	0.194	0.174	0.070	0.156	0.064
Al^{IV}	1.746	1.705	1.681	1.504	1.602	1.550	1.676	1.869	1.691	1.447
Al^{VI}	0.272	0.377	0.347	0.464	0.319	0.414	0.337	0.428	0.410	0.444
Cr	0.000	0.004	0.000	0.000	0.009	0.000	0.002	0.001	0.010	0.002
Fe^{3+}	0.534	0.501	0.510	0.355	0.346	0.305	0.416	0.672	0.443	0.419
Fe^{2+}	2.008	2.143	1.870	2.014	2.180	2.266	2.555	2.334	1.975	1.876
Mn	0.101	0.109	0.063	0.044	0.044	0.042	0.087	0.061	0.070	0.064
Mg	1.983	1.817	2.126	2.071	1.921	1.827	1.512	1.477	1.993	2.148
Ca	1.896	1.894	1.852	1.825	1.928	1.896	1.823	1.907	1.879	1.962
Na	0.426	0.442	0.416	0.371	0.299	0.280	0.454	0.442	0.406	0.351
K	0.324	0.297	0.258	0.232	0.277	0.274	0.307	0.285	0.240	0.143
Na(A)	0.370	0.386	0.337	0.278	0.260	0.224	0.360	0.392	0.341	0.331
$Mg/(Mg+Fe^{2+})$	0.497	0.459	0.532	0.507	0.468	0.446	0.372	0.388	0.502	0.534
Fe^{3+}/Fe^{2+}	0.266	0.234	0.273	0.176	0.159	0.135	0.163	0.288	0.224	0.223

* Total Fe as FeO.
[†] Retrograde mineral.

4.3. *Plagioclase*

In general, plagioclase shows a moderate compositional zoning with a broad plateau of Ca in the profile (Table 1). In sp. 85012808, plagioclase in direct contact with fine aggregates of epidote is An_{19}, while a core part is up to An_{35}.

4.4. *Garnet*

Tiny grains of garnet rarely occur in sp. 85012812. The garnets are highly resorbed and contain high MnO (8.94 wt%) and CaO (11.42 wt%). In sp. 85011503E, poikilitic garnet in contact with ortho- and clinopyroxenes shows a distinct reverse zoning.

4.5. *Epidote*

Epidote is found in many specimens except the opx-bg. rocks, although its amount varies from specimen to specimen. Fine epidote grains generally occur with quartz

Table 3 (continued).

Specimen No.	85011201				85011503C		85011503E		
	core	rim	cum-ming-tonite	Man-tle**	core	rim	core	rim	cum-ming-tonite
Analysis No.	120	119	203*	112	215	216	504	147	315*
SiO_2	39.99	40.44	52.81	38.84	41.96	41.12	40.85	40.22	44.34
TiO_2	2.02	1.84	0.01	0.04	2.33	2.30	2.10	0.92	0.17
Al_2O_3	12.38	12.14	0.72	17.26	11.38	11.92	11.35	12.50	0.98
Cr_2O_3	0.00	0.03	0.00	0.04	0.09	0.14	0.00	0.05	0.00
FeO*	18.61	17.87	24.97	19.61	17.77	17.01	21.01	21.77	39.50
MnO	0.22	0.24	1.01	0.20	0.25	0.19	0.14	0.12	0.95
MgO	8.75	9.28	16.47	6.71	9.89	9.44	7.49	7.18	10.41
CaO	11.24	11.38	0.46	11.33	11.38	11.65	11.08	10.81	0.42
Na_2O	1.44	1.18	0.07	1.19	1.59	1.48	1.43	1.27	0.00
K_2O	1.82	1.73	0.03	1.03	1.89	1.91	1.87	1.75	0.00
Total	96.47	96.13	96.55	96.24	98.53	97.16	97.32	96.57	96.77
On the basis of 23 oxygens									
Si	6.156	6.204	7.899	5.916	6.307	6.276	6.310	6.220	7.260
Ti	0.234	0.212	0.101	0.005	0.263	0.264	0.244	0.107	0.740
Al^{IV}	1.844	1.796	0.025	2.084	1.693	1.724	1.690	1.780	0.000
Al^{VI}	0.402	0.399	0.001	1.014	0.323	0.420	0.376	0.498	0.021
Cr	0.000	0.004	0.000	0.005	0.011	0.017	0.000	0.006	0.000
Fe^{3+}	0.343	0.418	—	0.666	0.186	0.051	0.206	0.558	—
Fe^{2+}	2.053	1.874	3.123	1.832	2.048	2.120	2.508	2.257	5.409
Mn	0.029	0.031	0.128	0.026	0.032	0.025	0.018	0.016	0.132
Mg	2.008	2.122	3.672	1.524	2.216	2.148	1.725	1.655	2.541
Ca	1.854	1.870	0.074	1.849	1.833	1.905	1.834	1.791	0.074
Na	0.430	0.351	0.020	0.351	0.463	0.438	0.428	0.381	0.000
K	0.357	0.339	0.006	0.200	0.362	0.372	0.369	0.345	0.000
Na(A)	0.352	0.282	—	0.271	0.374	0.387	0.340	0.270	—
$Mg/(Mg+Fe^{2+})$	0.494	0.531	0.540	0.454	0.520	0.503	0.408	0.423	0.320
Fe^{3+}/Fe^{2+}	0.167	0.223	—	0.364	0.091	0.024	0.082	0.247	—

* Total Fe as FeO. ** Mantle of cummingtonite.

at the fringe of green to bluish green hornblende and yellowish brown biotite (Plate 3b). In some cases, epidote makes aggregates with fine-grained chlorite. In sps. 84021912 and 85012808 which contain a few modal percent of epidote, two modes of occurrence of epidote are observed under the microscope: one is fine grains or aggregates, and the other is subhedral grains up to 0.2 mm in diameter (Plate 3b and 3c). However, the microprobe analysis shows a narrow range of chemical compositions X_{ps} $(Fe^{3+}/(Fe^{3+}+Al))=0.27–0.29$ in both cases. Moreover, both kinds of epidote are intimately associated with green to bluish green hornblende. Thus, all these features suggest secondary origin of epidote.

4.6. *Biotite*

Biotite occurs in all specimens analyzed. In the opx-bg. rocks, fine Ti-rich biotite (TiO_2 up to 4 wt%) occurs very rarely in contact with ilmenite, orthopyroxene and hornblende. A part of orthopyroxene is also replaced by biotite associated with

Table 4. Representative microprobe analyses of garnet.

Specimen No.	85012812	85011503E	
	fine	core	rim**
Analysis No.	401	155	152
SiO_2	37.11	37.80	37.08
TiO_2	0.03	0.00	0.03
Al_2O_3	19.98	20.51	20.60
FeO*	21.25	28.77	29.41
MnO	8.94	1.78	2.16
MgO	0.70	3.18	2.68
CaO	11.42	7.61	7.33
Total	99.42	99.66	99.28
On the basis of 12 oxygens			
Si	3.005	3.017	2.987
Al^{IV}	0.000	0.000	0.013
Al^{VI}	1.911	1.946	1.943
Ti	0.002	0.000	0.002
Fe	1.439	1.920	1.981
Mn	0.613	0.121	0.147
Mg	0.085	0.379	0.321
Ca	0.991	0.650	0.632
Mg/(Mg+Fe)	0.056	0.165	0.139

* Total Fe as FeO.
** next to clinopyroxene.

Table 5. Representative microprobe analyses of epidote.

Specimen No.	85012808			85012812B	84021915
	very fine	core	rim	fine	fine
Analysis No.	312	115	114	174	301
SiO_2	37.20	37.45	37.35	37.20	36.91
TiO_2	0.04	0.05	0.09	0.08	0.11
Al_2O_3	22.94	21.90	22.30	22.76	22.67
Fe_2O_3	13.60	13.92	13.05	14.05	13.67
MnO	0.40	0.36	0.50	0.22	0.30
MgO	0.02	0.02	0.01	0.02	0.01
CaO	22.57	22.75	22.54	22.85	22.33
Total	96.76	96.47	95.85	97.18	96.00
On the basis of 25 oxygens					
Si	6.002	6.073	6.078	5.988	6.001
Ti	0.005	0.006	0.010	0.010	0.014
Al	4.362	4.185	4.277	4.317	4.344
Fe^{3+}	1.651	1.698	1.598	1.702	1.673
Mn	0.055	0.049	0.069	0.030	0.042
Mg	0.006	0.006	0.002	0.004	0.003
Ca	3.901	3.952	3.930	3.940	3.891
Total	15.989	15.970	15.965	15.992	15.967
$Fe^{3+}/(Fe^{3+}+Al)$	0.275	0.289	0.272	0.283	0.278

Table 6. Representative chemical compositions of biotite.

Specimen No.	85012808		85012811		85012812B		84021912		84021915		85011503C	85011503E	
	core	rim	core	rim	core	rim	core	rim	core	rim	fine	fine	fine
Analysis No.	324	221	205	202	119	116	101	102	324	325	205[1)]	104[2)]	210[3)]
SiO_2	36.15	36.39	36.13	36.43	36.69	36.26	34.57	34.98	36.15	36.23	37.58	36.19	35.52
TiO_2	1.88	1.66	1.78	2.08	2.43	2.24	3.53	3.39	2.17	2.23	4.97	3.47	4.42
Al_2O_3	15.02	14.97	16.09	15.93	15.47	15.34	15.05	15.37	15.39	15.55	13.72	13.66	16.28
Cr_2O_3	0.02	0.00	0.02	0.01	0.00	0.02	0.00	0.01	0.08	0.07	0.08	0.03	0.02
FeO*	18.61	18.16	18.96	18.65	21.47	19.71	27.86	27.68	17.53	18.12	18.01	21.25	21.09
MnO	0.60	0.57	0.15	0.05	0.28	0.37	0.48	0.40	0.25	0.30	0.11	0.07	0.03
MgO	12.10	12.20	12.38	11.97	10.67	10.92	5.34	5.27	11.73	11.59	12.50	10.89	8.64
CaO	0.02	0.03	0.00	0.01	0.00	0.00	0.00	0.03	0.03	0.05	0.07	0.02	0.03
Na_2O	0.07	0.00	0.15	0.17	0.09	0.02	0.02	0.01	0.07	0.02	0.06	0.00	0.00
K_2O	9.34	9.28	9.00	8.72	8.98	9.42	8.81	8.87	9.11	9.34	9.64	8.89	9.19
Total	93.81	93.27	94.65	94.03	96.07	94.29	95.66	96.00	92.52	93.50	96.73	94.46	95.22
On the basis of 22 oxygens													
Si	5.606	5.655	5.531	5.590	5.594	5.613	5.497	5.526	5.635	5.609	5.622	5.626	5.467
Al^{IV}	2.394	2.345	2.469	2.410	2.406	2.387	2.503	2.474	2.365	2.391	2.378	2.374	2.533
Al^{VI}	0.351	0.397	0.434	0.470	0.373	0.412	0.318	0.386	0.463	0.446	0.042	0.129	0.420
Ti	0.219	0.194	0.205	0.240	0.279	0.260	0.422	0.403	0.254	0.260	0.559	0.405	0.511
Cr	0.003	0.000	0.002	0.001	0.000	0.002	0.000	0.001	0.010	0.009	0.009	0.004	0.003
Fe	2.414	2.360	2.427	2.393	2.737	2.551	3.704	3.657	2.286	2.346	2.254	2.762	2.715
Mn	0.079	0.075	0.020	0.007	0.036	0.049	0.065	0.053	0.033	0.039	0.013	0.009	0.004
Mg	2.798	2.827	2.825	2.738	2.426	2.520	1.266	1.241	2.725	2.675	2.789	2.523	1.984
Ca	0.003	0.004	0.000	0.002	0.000	0.000	0.000	0.004	0.005	0.008	0.011	0.003	0.005
Na	0.020	0.001	0.043	0.051	0.025	0.005	0.006	0.004	0.020	0.006	0.017	0.000	0.000
K	1.848	1.841	1.757	1.707	1.747	1.860	1.788	1.788	1.812	1.845	1.841	1.762	1.805
Mg/(Mg+Fe)	0.537	0.545	0.538	0.534	0.470	0.497	0.255	0.253	0.544	0.534	0.553	0.477	0.422

* Total Fe as FeO.

1) next to hornblende, 2) next to garnet, 3) next to orthopyroxene.

Table 7. Representative chemical compositions of Fe-Ti minerals.

Specimen No.	85012808	85012811	84021912	85011201		85011503E	
	Mag	Mag	Hem	Mag	Il	Mag	Il
Analysis No.	233	109	110	302	212	131	302
SiO_2	0.10	0.29	0.06	0.00	0.02	0.01	0.00
TiO_2	0.00	0.04	1.29	0.58	49.35	0.39	50.68
Al_2O_3	0.00	0.00	0.12	0.28	0.01	0.58	0.02
Cr_2O_3	0.01	0.11	0.00	0.13	0.00	0.01	0.03
FeO*	92.43	90.60	87.95	91.95	48.96	91.08	48.12
MnO	0.06	0.10	0.06	0.06	0.84	0.04	0.65
MgO	0.00	0.01	0.01	0.03	0.24	0.03	0.35
CaO	0.00	0.18	0.04	0.00	0.03	0.09	0.00
Total	92.60	91.34	89.53	93.02	99.44	92.23	99.83
Recalculated analyses							
Fe_2O_3	68.36	66.77	96.52	67.24	6.52	66.80	4.24
FeO	30.91	30.51	1.08	31.43	43.09	30.96	44.30
Total	99.44	98.02	99.18	99.75	100.09	98.91	100.26
R_2O_3	0.00	0.00	97.29	0.00	6.21	0.00	4.08
Usp	0.39	1.28	0.00	1.68	0.00	1.17	0.00
O	4.000	4.000	6.000	4.000	6.000	4.000	6.000
Si	0.004	0.012	0.003	0.000	0.001	0.000	0.000
Ti	0.000	0.001	0.052	0.017	1.875	0.011	1.918
Al	0.000	0.000	0.008	0.013	0.001	0.026	0.001
Cr	0.000	0.003	0.000	0.004	0.000	0.000	0.001
Fe^{3+}	1.992	1.971	3.883	1.950	0.248	1.950	0.161
Fe^{2+}	1.001	1.001	0.048	1.013	1.820	1.005	1.865
Mn	0.002	0.003	0.003	0.002	0.036	0.001	0.028
Mg	0.000	0.001	0.001	0.001	0.018	0.002	0.026
Ca	0.000	0.007	0.002	0.000	0.002	0.004	0.000

* Total Fe as FeO.

quartz. In the other rocks, yellowish to pale brown biotite is poor in Ti (TiO_2 1–2 wt%) and shows no distinct chemical zoning.

4.7. Other minerals

Quartz is contained in all specimens analyzed. K-feldspar (microcline) is found only in sp. 85012812B. Sphene is found in many specimens except for the opx-bg. rocks. Opaque minerals are ilmenite, hematite, magnetite and sulphide minerals. In the opx-free rocks, magnetite is the only opaque mineral, while ilmenite and magnetite are common in the opx-bg. rocks. Ilmenite generally has fine exsolution lamellae of hematite. Muscovite, chlorite and calcite appear to be of secondary origin.

5. Discussion

5.1. Mineral equilibria and metamorphic conditions

The specimens described here are highly altered during the later retrograde metamorphism. However, the profiles of the zoned mineral grains such as pyroxenes, garnet and plagioclase generally show broad peaks and troughs of elements distributions, suggesting chemical equilibrium under the peak metamorphic conditions. Therefore, chemical compositions of core portions of these zoned minerals are used to estimate the peak metamorphic conditions.

Mineral assemblages of the northern part of the northern group (Brattnipane) clearly show the metamorphic conditions up to the granulite facies because of common occurrence of orthopyroxene, whereas orthopyroxene has not been found in the southern part of the northern group (Fig. 1). First of all, the paragenetic relation of opx-bg. rocks will be examined.

In general, the stability relations among pyroxenes, amphiboles, garnet and plagioclase in quartz-bearing basic to intermediate metamorphic rocks are presented in the system Al_2O_3-MgO-FeO-CaO-Na_2O (SHIRAISHI *et al.*, 1984). The Na content of calcic amphibole is closely related to that of plagioclase, as will be discussed later. Figure 2 shows the chemographic relations among coexisting pyroxenes, calcic amphibole and garnet. Taking the analytical errors and non-ideality of amphibole solid solutions into account, these diagrams strongly suggest equilibrium relationships of the minerals at the peak of metamorphism. Sp. 85011503E has an invariant assemblage of orthopyroxene-clinopyroxene-garnet-calcic amphibole-plagioclase at given metamorphic conditions in the system Al_2O_3-MgO-FeO-CaO-Na_2O. In Fig. 2,

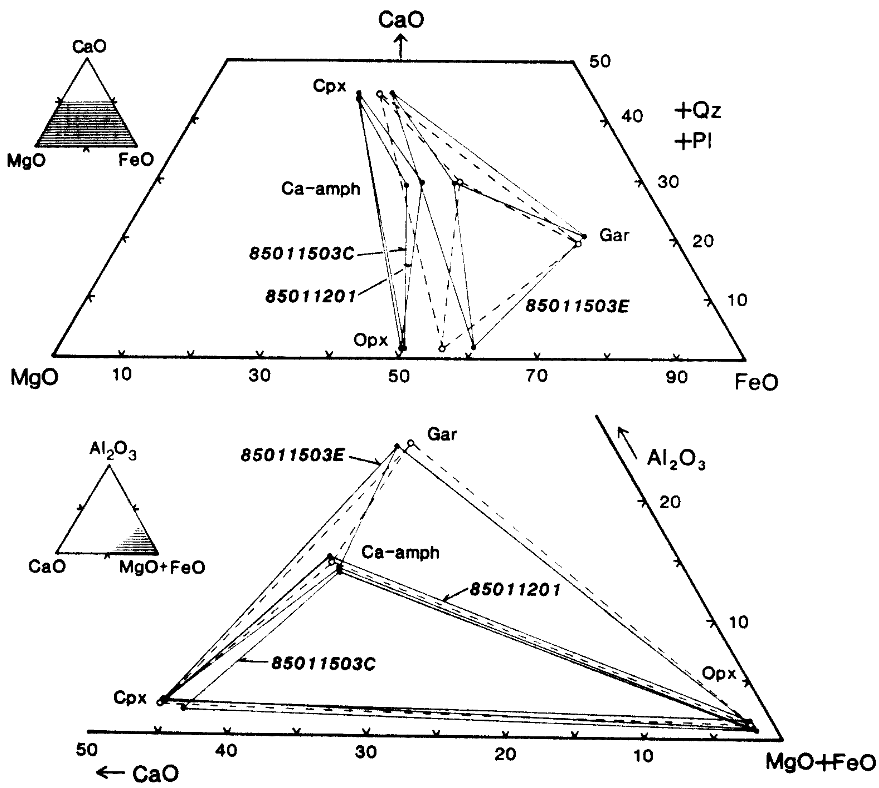

Fig. 2. CaO-MgO-FeO (a) and Al_2O_3-CaO-(MgO+FeO) (b) diagrams showing chemographic relations among minerals from orthopyroxene-bearing gneisses. Open circles connected with broken lines show the compositions of minerals in a granulite (sp. 69020613) from the Skallen district, Lützow-Holm Bay region (data from SUZUKI, 1983).

chemographic relations of the same assemblage in the granulite facies rock from the Skallen district of the Lützow-Holm Bay region are also plotted. Compatible relationships among coexisting minerals from both regions suggest that the metamorphic conditions are similar to each other.

5.2. Compositions of calcic amphibole as a key of the metamorphic grade

5.2.1. Compositions of calcic amphibole coexisting with or without orthopyroxene

In the southern part of the northern group (northern ridges of Wideröefjellet and Walnumfjellet), the basic to intermediate gneisses have rather simple assemblages without orthopyroxene, and the metamorphic grade may belong to the amphibolite facies. However, the amphibolite facies occupies a wide range of *P-T* space. Chemical compositions of calcic amphiboles which are ubiquitous in all the specimens, may be a good indicater of the metamorphic grade.

Calcic amphiboles of the opx-bg. rocks from the northern part are slightly more pargasitic and much more titanian than those of the opx-free rocks from the southern part, clearly indicating a higher temperature condition of the opx-bg. rocks (SPEAR, 1981a).

The bulk chemical compositions and oxidation states of the present specimens are not available. It is noteworthy that opx-free rocks characteristically contain sphene but not ilmenite as titanian accessory minerals, whereas the opx-bg. rock contains ilmenite but not sphene. The strong f_{O_2} dependence of the upper thermal stability limit of sphene was indicated by SPEAR (1981a). For the estimation of Fe^{3+}, the results of the microprobe analyses have been recalculated from stoichiometric constrains following the procedure of STOUT (1972) and BRADY (1974) (Table 3). Difference of Fe^{3+}/Fe^{2+} in the core portions of calcic amphibole between the two groups (0.16–0.27 in the opx-free rocks and 0.08–0.17 in the opx-bg. rocks) suggests decreasing f_{O_2} from the opx-free rocks to the opx-bg. rocks. This is consistent with the reaction suggested by SPEAR (1981a) such as:

$$Hb_1+Pl_1+Sph+Ti\text{-}hem=Hb_2+Pl_2+Il+O_2+H_2O\ ,$$

(where Hb_2 is more Fe-, Ti-, and pargasite-rich than Hb_1) for the consumption of sphene.

SHIRAISHI *et al.* (1984) discussed the first appearance of orthopyroxene in the progressive metamorphic sequence in the Prince Olav Coast, eastern Queen Maud Land. Although there are many reactions to form orthopyroxene, they inferred the following reaction in rocks relatively rich in Al and Fe^{2+}.

$$Tsch+Qz=Opx+An+H_2O\ . \qquad (1)$$

Figure 3 shows the chemical compositions of calcic amphibole in terms of Na *vs.* $Al^{VI}+Fe^{3+}+Ti$. The two groups with or without orthopyroxene are separately plotted although part of them seems to be overlapped. Figure 3 illustrates that the above reaction (1) is just the case of the present region. In conclusion, the metamorphic conditions of the southern part of the northern group may be not far from the granulite facies but the uppermost amphibolite facies, and the f_{O_2} is lower in the northern part than in the southern part.

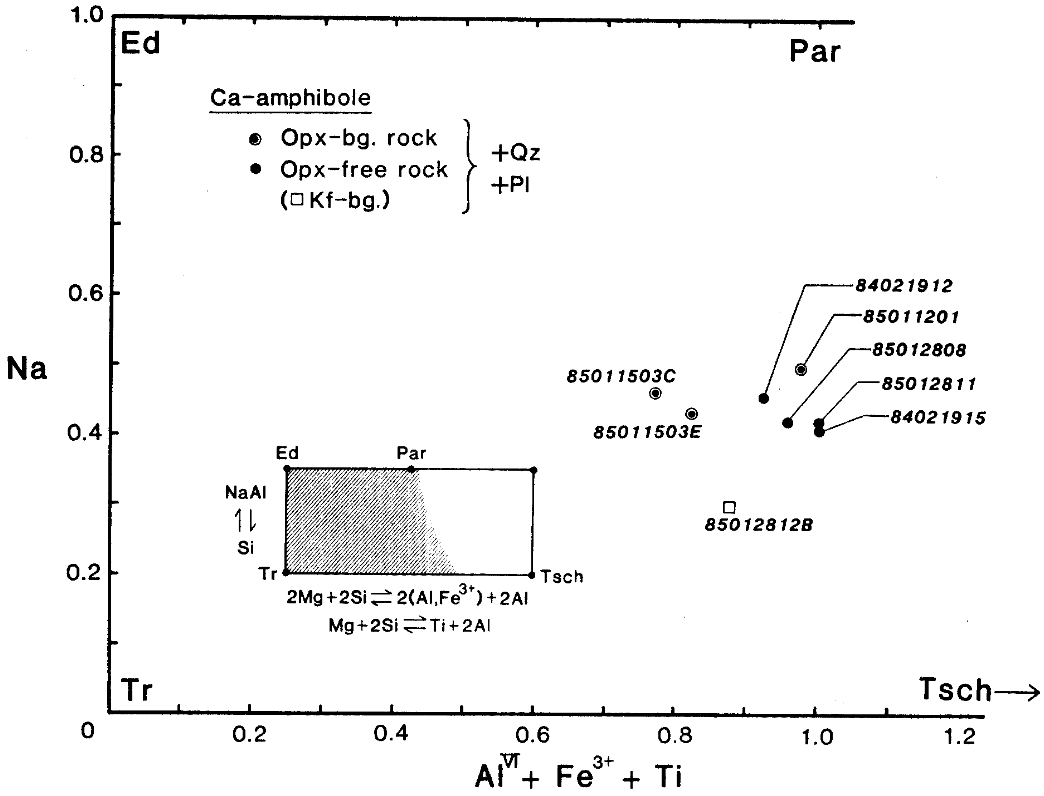

Fig. 3. Na vs. Al^{VI} diagram for calcic amphibole. A square indicates a K-feldspar-bearing rock (sp. 85012812B).

5.2.2. Na partitioning between calcic amphibole and plagioclase

Since all specimens described here coexist with plagioclase and quartz, partitioning of Na between plagioclase and the A-site of calcic amphibole is described by the relation:

$$\underset{\text{albite}}{NaAlSi_3O_8}+\underset{\text{tremolite}}{Ca_2Mg_5Si_8O_{22}(OH)_2}=\underset{\text{edenite}}{NaCa_2Mg_5AlSi_7O_{22}(OH)_2}+\underset{\text{quartz}}{4SiO_2}\,. \quad (2)$$

Reaction (2) proceeds to the right with increasing temperature (SPEAR, 1981b). Figure 4 shows the plots of $X_{Na(A)}$ ($=Na(A)/(NA(A)+\square(A))$, where $\square(A)$ is A-site vacancy) in calcic amphibole *vs.* X_{Ab} (mole% of albite) in plagioclase with hypothetical contours by SPEAR (1981b). The amount of Na(A) was obtained from the recalculation of microprobe data in the same fashion with Fe^{3+} estimation following the procedure mentioned above. Figure 4 clearly shows that the opx-bg. rocks are plotted in the higher grade area than the other rocks. However, the stratigraphic positions of the specimens examined are not necessarily reflected on the plots. It may result from uncertainty of the amphibole composition and non-ideality of the amphibole and plagioclase solid solutions. Figure 4 also suggests the metamorphic grade of the southern part of the northern group belongs to the upper amphibolite facies.

On the other hand, equilibrium relations between calcic amphibole and plagioclase are also described by reactions containing glaucophane molecule. However,

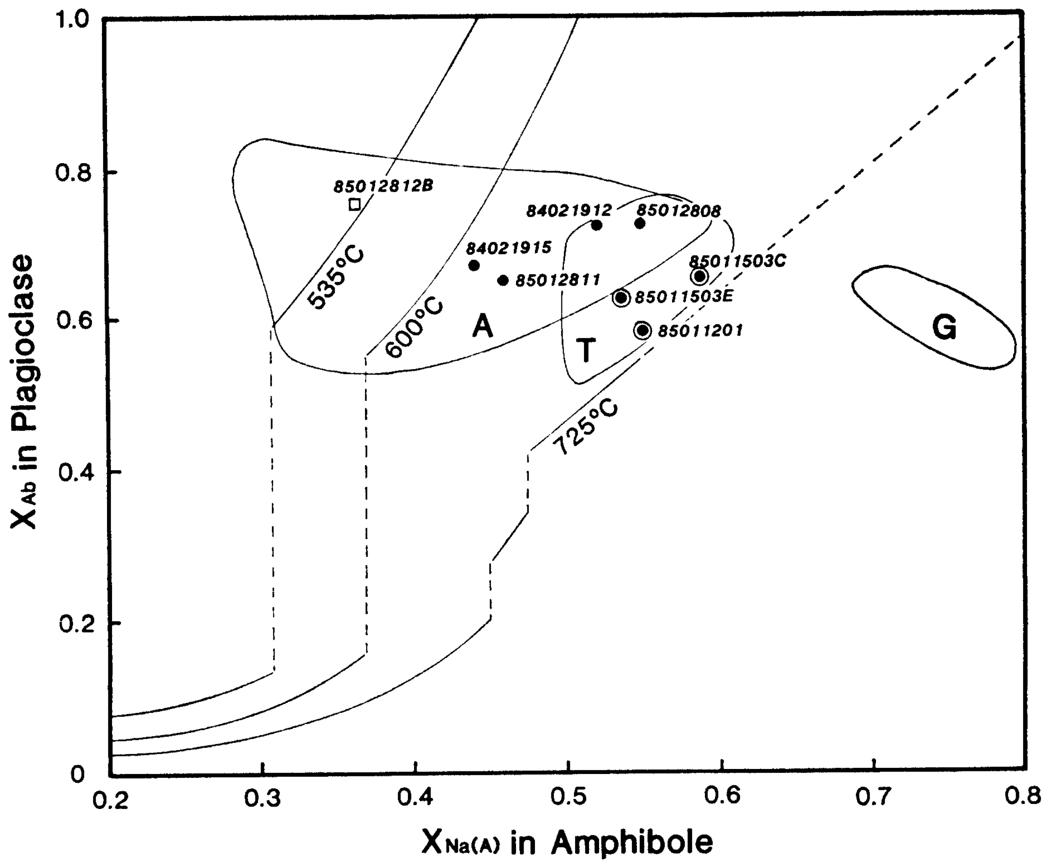

Fig. 4. *Plots of $X_{Na(A)}$ in calcic amphibole vs. X_{Ab} in coexisting plagioclase. Hypothetical contours of 725°C and 600°C after* SPEAR *(1981a, b) are shown for reference. Areas "A", "T" and "G" indicate compositional fields for rocks from the amphibolite facies zone, the transitional zone and the granulite facies zone in the Prince Olav Coast and Lützow-Holm Bay region, respectively (*SHIRAISHI*, 1986). Symbols are the same as Fig. 3.*

Table 8. Two-pyroxene geothermometry.

Specimen No.		X_{Mg}^{Cpx}	X_{Mg}^{Opx}	K_D	Temperature(°C)			
					T_1	T_2	T_3	T_4
85011201	core	(326) 0.607	(331) 0.496	1.569	837	883	782	910
	rim	(325) 0.629	(333) 0.493	1.742	780	800	631	793
85011503C	core	(204) 0.611	(201) 0.491	1.626	863	924	847	867
	rim	(203) 0.639	(202) 0.476	1.947	809	845	719	692
85011503E	core	(163) 0.520	(212) 0.395	1.659	807	852	708	845
	rim	(304) 0.537	(305) 0.383	1.876	801	844	687	723

( ): Analysis point number.

X_{Mg}=Mg/(Mg+Fe), K_D=(Fe/Mg)$_{Opx}$/(Fe/Mg)$_{Cpx}$.

T_1: WOOD and BANNO (1973), T_2: WELLS (1977), T_3: Solvus by KRETZ (1982), T_4: K_D by KRETZ (1982).

Table 9. Garnet-pyroxene geothermometry and geobarometry of specimen 85011503E.

A) Geothermometry

Pairs	X_{Mg}^{Gar}	X_{Mg}^{Opx}	X_{Mg}^{Cpx}	ln K_{D1}	ln K_{D2}	P (kb)	Temperature (°C)		
							T_1	T_2	T_3
core	(155)	(212)		1.1946		6		693	779
	0.165	0.395				8		703	792
core	(155)		(163)		1.6875	6	779		
	0.165		0.520			8	785		
rim	(152)		(151)		2.1784	6	649		
	0.139		0.589			8	654		

( ): Analysis point number.
X_{Mg}: Mg/(Mg+Fe).
K_{D1}: (Fe/Mg)Gar/(Fe/Mg)Cpx, K_{D2}: (Fe/Mg)Gar/(Fe/Mg)Cpx.
T_1: Ellis and Green (1979), T_2: Harley (1984a), T_3: Sen and Bhattacharya (1984).

B) Geobarometry

Pairs	Gar	Opx	Cpx	Pl (An)	T (°C)	Pressure (kb)			
						P_1	P_2	P_3	P_4 [log K]
core	(155)	(212)		35	800	14.81	12.15	8.59	~8.5 [0.471]
core	(155)		(163)	35	800			7.18	
rim	(152)	(313)		35	650	9.59	10.94	6.56	~6.6 [0.368]
rim	(152)		(151)	35	650			4.58	

( ): Analysis point numbers.
$K = a_{An}^3 \cdot a_{Fs}^3 / a_{Gr} \cdot a_{Alm}^2$.
P_1: Harley and Green (1982), P_2: Harley (1984b), P_3: Perkins and Newton (1981), P_4: Bohlen *et al.* (1983).

they are not suitable for the present specimens because Na(M4) is calculated extremely low.

5.3. *Geothermometry and geobarometry*

Geothermo-barometers are adopted to estimate *P-T* conditions during the granulite facies metamorphism. Tables 8 and 9 show the results of calculation. To take the peak metamorphic conditions, core parts of the coexisting minerals are used for calculation.

Three pairs of two-pyroxenes show temperatures between 800 and 860°C by Wood and Banno's (1973) thermometer, and between 850 and 920°C by Wells' (1977) thermometer. Two methods by Kretz (1982) give a large temperature range over 130°C. Sp. 85011503E containing garnet, orthopyroxene, clinopyroxene, plagioclase and quartz enables us to apply some garnet-pyroxenes geothermo-barometries (Table 9). Calculated temperatures between 780 and 790°C except those by Harley's (1984a) thermometer are consistent with each other at 6 to 8 kb although somewhat lower than two-pyroxene temperature. As is well-known, Wells' thermometer gives scattered and high values for granulites (ESSENE, 1982). Moreover, WOOD (1975) stated that it is reliable to reduce 50°C from the calculation after WOOD and BANNO (1973). Although there remains some ambiguity, the peak metamorphic temperature inferred from core compositions is around 800°C.

On the other hand, calculated temperatures using rim compositions in direct contact with each other yield around 800°C for two-pyroxene pairs and 650°C for a garnet-clinopyroxene pair.

For the geobarometry, there are no petrographic evidence to support the high pressures calculated by HARLEY and GREEN (1982) and HARLEY (1984b). Garnet and pyroxene pairs from Fe-rich granulite may not be suitable for these methods. Garnet-orthopyroxene barometry by PERKINS and NEWTON (1981) and BOHLEN *et al.* (1983) is consistent and indicates around 8.5 kb at 800°C. However, the garnet-clinopyroxene barometry by PERKINS and NEWTON (1981) yields a lower pressure of 7.2 kb.

In conclusion, we take around 800°C and 7–8.5 kb as the possible peak metamorphic conditions. These conditions are similar to those of southern Sôya Coast of the Lützow-Holm Bay region (MOTOYOSHI and SHIRAISHI, 1985; MOTOYOSHI, 1986; HIROI *et al.*, 1987). This result is consistent with the prediction by chemographic relations of minerals between the two regions mentioned above.

5.4. *Retrograde metamorphism in the western part of the Sør Rondane Mountains*

Retrograde textures are widespread in the metamorphic rocks from the present area. Cummingtonite surrounding orthopyroxene and biotite replacing orthopyroxene observed in rocks from the northern part (Brattnipane) can be interpreted as retrograde products formed through the reactions:

$$\mathrm{Opx+Qz+H_2O=Cum}\ ,$$

$$\mathrm{Opx+Kf+H_2O=Bi+Qz}\ .$$

Moreover, cummingtonite in sp. 85011201 is also surrounded by a mantle of tschermakitic hornblende. The possible raction is

$$\mathrm{Cum+An+H_2O=Tsch+Qz}\ .$$

Much of epidote found in the gneisses from the northern group is probably secondary in origin. Even though it may appear to be primary by textural criteria, the chemical compositions are not different from those of the apparently secondary one. The mode of occurrence of epidote described in the previous section suggests that it is a product of hydration reactions as follows:

$$\mathrm{Ca\text{-}amph+H_2O=Epi+Chl+Qz}\ ,$$

$$\mathrm{Ca\text{-}amph+An+H_2O=Epi+Qz}\ .$$

The mode of field occurrence suggests these reactions caused mainly by granite intrusion but also by mylonitization.

6. Conclusions

(1) Mineral assemblages of basic to intermediate gneisses from the northern group of the western Sør Rondane Mountains show the peak metamorphic grade up to the granulite facies. Judging from the variations of chemical compositions of calcic amphiboles as well as mineral assemblages, the peak metamorphic grade in the southern part of the northern group (northern ridges of Wideröefjellet and Walnumfjellet) belongs to the upper amphibolite facies. However, gradual decrease of metamorphic grade from north to south has not been detected.

(2) Possible peak metamorphic conditions of the granulite facies rocks from Brattnipane are around 800°C and 7–8.5 kb on the basis of various geothermobarometries.

(3) Various hydration reactions caused probably by granite activity and mylonitization formed secondary cummingtonite, tschermakitic hornblende, epidote and chlorite.

Acknowledgments

We are much indebted to M. ASAMI of Okayama University, Y. HIROI of Chiba University and Y. MOTOYOSHI of the University of New South Wales for helpful criticism of the early version of the manuscript. We wish to thank K. YANAI and H. KOJIMA for their support and assistance in the microprobe study.

References

BOHLEN, S. R., WALL, V. J. and BOETTCHER, A. L. (1983): Geobarometry in granulites. Kinetics and Equilibrium in Mineral Reactions, ed. by S. K. SAXENA. New York, Springer, 141–171.

BRADY, J. B. (1974): Coexisting actinolite and hornblende from west-central New Hampshire. Am. Mineral., **59**, 529–535.

ELLIS, D. J. and GREEN, D. H. (1979): An experimental study of the effect of Ca upon garnet-clinopyroxene exchange equilibria. Contrib. Mineral. Petrol., **71**, 13–22.

ESSENE, E. J. (1982): Geologic thermometry and barometry. Rev. Mineral., **10**, 153–206.

HARLEY, S. L. (1984a): An experimental study of the partitioning of Fe and Mg between garnet and orthopyroxene. Contrib. Mineral. Petrol., **86**, 359–373.

HARLEY, S. L. (1984b): The solubility of alumina in orthopyroxene coexisting with garnet in FeO-MgO-Al_2O_3-SiO_2 and CaO-FeO-MgO-Al_2O_3-SiO_2. J. Petrol., **25**, 665–696.

HARLEY, S. L. and GREEN, D. H. (1982): Garnet-orthopyroxene barometry for granulites and peridotites. Nature, **300**, 679–701.

HIROI, Y., SHIRAISHI, K., MOTOYOSHI, Y. and KATSUSHIMA, T. (1987): Progressive metamorphism of calc-silicate rocks from the Prince Olav and Sôya Coasts, East Antarctica. Proc. NIPR Symp. Antarct. Geosci., **1**, 73–97.

KOJIMA, S. and SHIRAISHI, K. (1986): Note on the geology of the western part of the Sør Rondane Mountains, East Antarctica. Mem. Natl Inst. Polar Res., Spec. Issue, **43**, 116–131.

KRETZ, R. (1982): Transfer and exchange equilibria in a portion of the pyroxene quadrilateral as deduced from natural and experimental data. Geochim. Cosmochim. Acta, **46**, 411–421.

MOTOYOSHI, Y. (1986): Prograde and progressive metamorphism of the granulite-facies Lützow-Holm Bay region, East Antarctica. Ph. D. thesis, Hokkaido Univ., 238 p.

MOTOYOSHI, Y. and SHIRAISHI, K. (1985): Petrography and geothermometry-geobarometry of Botnnuten, East Antarctica. Mem. Natl Inst. Polar Res., Spec. Issue, **37**, 127–146.

PERKINS, D. III and NEWTON, R. C. (1981): Charnockite geobarometers based on coexisting garnet-pyroxene-plagioclase-quartz. Nature, **292**, 144–146.

SEN, S. K. and BHATTACHARYA, A. (1984): An orthopyroxene-garnet thermometer and its application to the Madras charnockites. Contrib. Mineral. Petrol., **88**, 64–71.

SHIRAISHI, K. (1986): Geology and petrology of Late Proterozoic metamorphic complexes in eastern Queen Maud Land, East Antarctic Shield. D. Sc. thesis, Hokkaido Univ., 246 p.

SHIRAISHI, K., HIROI, H. and ONUKI, H. (1984): Orthopyroxene-bearing rocks from the Tenmondai and Naga-iwa Rocks in the Prince Olav Coast, East Antarctica; First appearance of orthopyroxene in progressive metamorphic sequence. Mem. Natl Inst. Polar Res., Spec. Issue, **34**, 126–144.

SPEAR, F. S. (1981a): An experimental study of hornblende stability and compositional variability in amphibole. Am. J. Sci., **281**, 697–734.

SPEAR, F. S. (1981b): Amphibole-plagioclase equilibria; An empirical model for the relation albite+tremolite=edenite+4 quartz. Contrib. Mineral. Petrol., **77**, 355–364.

STOUT, J. H. (1972): Phase petrology and mineral chemistry of coexisting amphiboles from Telemark, Norway. J. Petrol., **13**, 99–145.

SUZUKI, M. (1983): Preliminary note on the metamorphic conditions around Lützow-Holm Bay, East Antarctica. Mem. Natl Inst. Polar Res., Spec. Issue, **28**, 132–143.

VAN AUTENBOER, T. and LOY, W. (1972): Recent geological investigations in the Sør-Rondane Mountains, Belgicafjella and Sverdrupfjella, Dronning Maud Land. Antarctic Geology and Geophysics, ed. by R. J. ADIE. Oslo, Universitetsforlaget, 563–571.

WELLS, P. R. A. (1977): Pyroxene thermometry in simple and complex systems. Contrib. Mineral. Petrol., **62**, 129–139.

WOOD, B. J. (1975): The influence of pressure, temperature and bulk composition on the appearance of garnet in orthogneiss—an example from South Harris, Scotland. Earth Planet. Sci. Lett., **26**, 299–311.

WOOD, B. J. and BANNO, S. (1973): Garnet-orthopyroxene and orthopyroxene-clinopyroxene relationships in simple and complex systems. Contrib. Mineral. Petrol., **42**, 109–124.

(Received March 30, 1987; Revised manuscript received May 6, 1987)

a

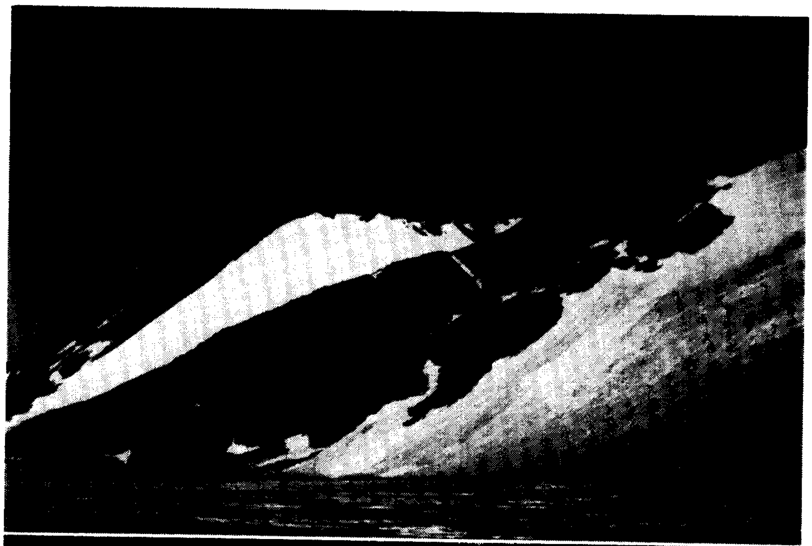

b

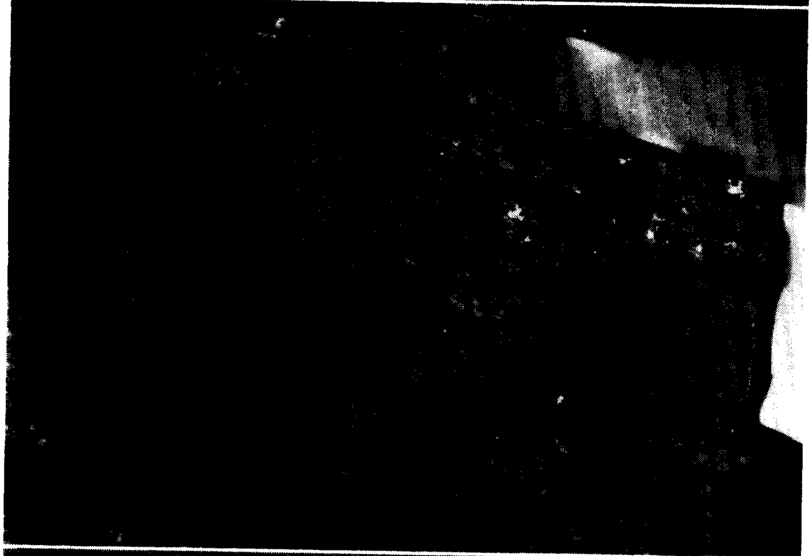

c

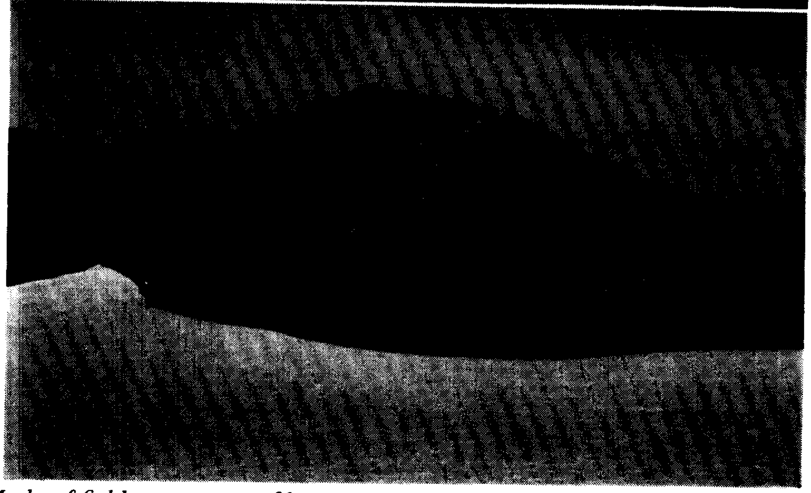

Plate 1. Mode of field occurrence of basic to intermediate gneisses from the northern group in the western part of the Sør Rondane Mountains.

a. Alternation of intermediate to basic gneisses, uniformly dipping southwards. (Northwestern corner of Brattnipane)

b. Finely banded intermediate gneiss (sp. 84021912)

c. Intermediate and basic gneisses intruded by subconcordant layers and dikes of granite. (Vengen, near the locality of sp. 85012812B)

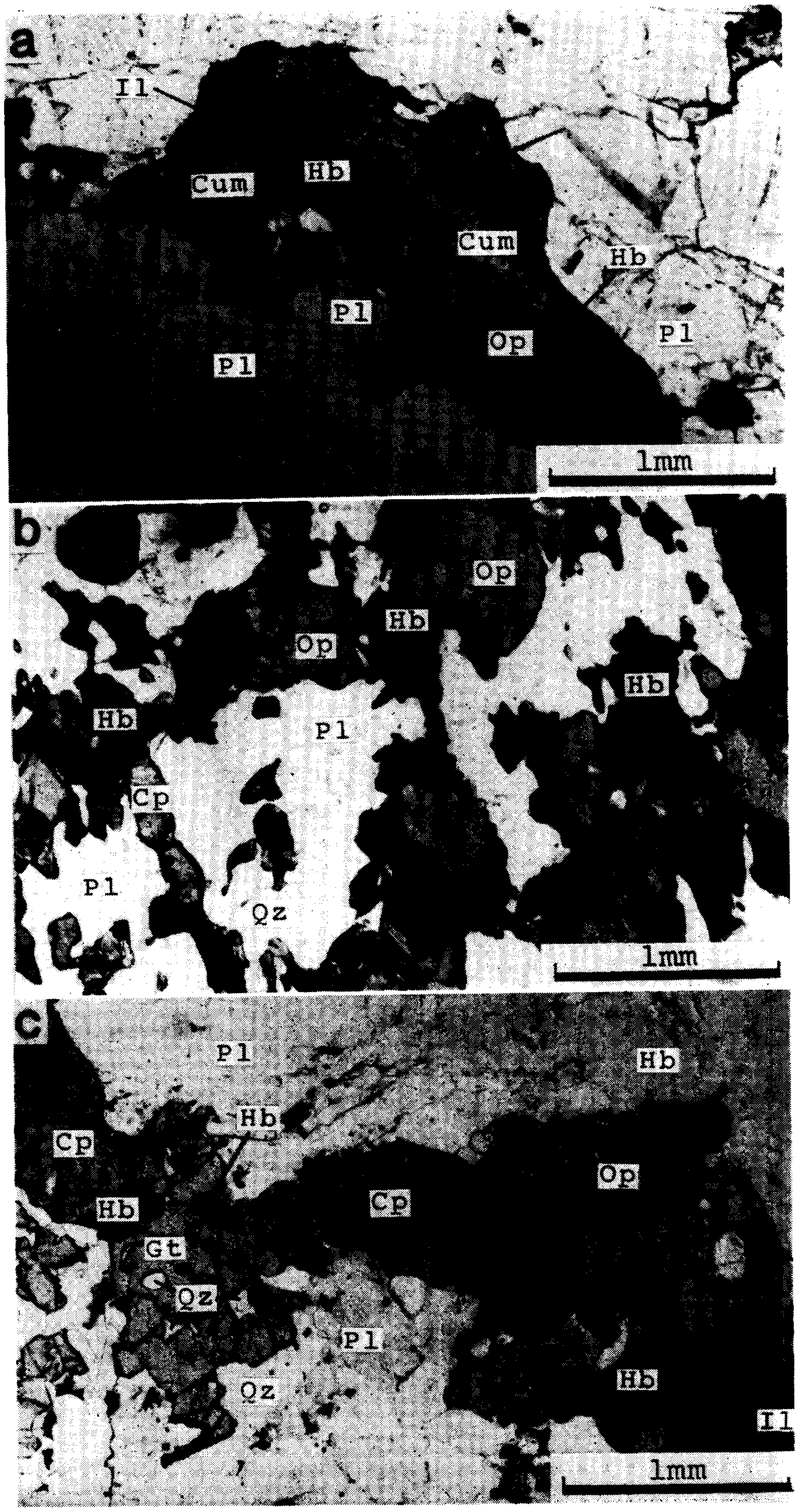

Plate 2. Photomicrographs of orthopyroxene-bearing gneisses.

a. Orthopyroxene mantled by retrograde cummingtonite which is also surrounded by bluish-green tschermakitic hornblende. (sp. 85011201)

b. Two-pyroxene amphibolite. (sp. 85011503C)

c. Garnet-hornblende-two-pyroxene gneiss. (sp. 85011503E)

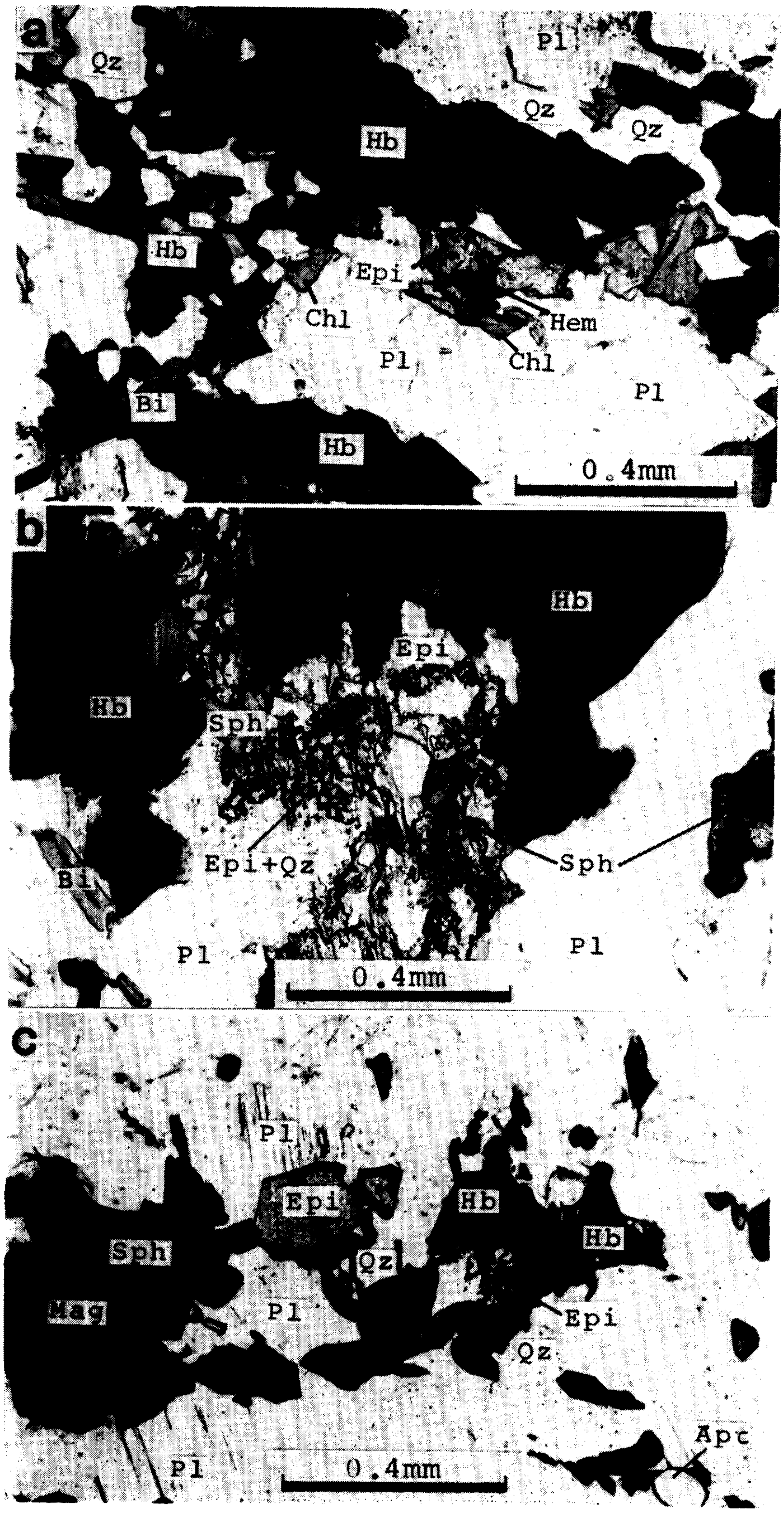

Plate 3. Photomicrographs showing mode of occurrence of epidote.

a. Epidote and chlorite in contact with hornblende. Note color zoning of hornblende. (sp. 84021915)

b. Epidote coexisting with hornblende and quartz. (sp. 85012808)

c. Subhedral epidote and fine aggregate of epidote. (sp. 84021912)